Investigating the Wound Healing Perspectives of Silver Nanoparticles Loaded Topical Nanogels

Ruchi Shivhare[1]*, Neelam Jain[2]

[1]*Research Scholar, Faculty of Pharmacy, Oriental University, Indore-453555, Madhya Pradesh, India
[2]Department of Pharmaceutics, Faculty of Pharmacy, Oriental University, Indore-453555, Madhya Pradesh, India

*Corresponding Author: Ruchi Shivhare
Address:Research Scholar, Faculty of Pharmacy, Oriental University, Indore-453555, Madhya Pradesh, India
Email id:shivharer4@gmail.com, Contact no: +91 9503640446,

ABSTRACT

The primary objective of the present investigation revolves around the development and evaluation of nanogel formulations by incorporating oleanolic acid-loaded silver nanoparticles. The formulation underwent a comprehensive assessment to evaluate its therapeutic attributes and topical delivery. The formulation was prepared by using carbopol 940 and triethanolamine. The parameters were analyzed as pH 5.5, viscosity 3500 cps, spreadability 6.9 g/cm/sec, and skin irritation tests showed no skin rashes. *Ex-vivo* drug release shows a slow release of the drug. There was 84.66% drug release in 12 hours. Additionally, Swiss albino rats were employed in this research to investigate the wound-healing capabilities of topical gel containing silver nanoparticles. Stability studies of the nanogel formulation were done. The results confirmed the spherical shape and uniform particle size of silver nanoparticles and the good stability of the nanogel. This study has provided a way for novel approaches to address wounds of various origins. The formulated topical gels loaded with silver nanoparticles exhibit promising prospects as wound healing agents. They are anticipated to enhance the natural wound healing process significantly and play a pivotal role in rat wound closure rate and epithelization. In comparison to the standard pharmaceutical agent betadine, the nanogel formulation exhibited equivalent efficacy. This discovery sheds light on the potential applications of nanoparticle-infused formulations in the conventional management of severe wound conditions, thereby revitalizing therapeutic principles within the field of modern medicine.

Keywords: silver nanoparticles, wound healing, nanogels, green synthesis.

1. INTRODUCTION

Following an injury, the body initiates a complex process known as wound healing, which aims to restore the integrity of the skin or affected organ [1]. Under normal circumstances, the epidermis and dermis of the skin function harmoniously to shield the body from environmental factors [2]. However, when this protective barrier is compromised due to injury or stress, the body's innate wound-healing response is activated [3]. This restorative process is initiated by growth factors, which employ autocrine, paracrine, and endocrine signaling mechanisms [4]. Various growth factors, such as platelet-derived growth factor (PDGF), epidermal growth factor (EGF), and fibroblast growth factor (FGF), contribute uniquely to different aspects of wound healing [5].

Numerous commercial wound healing treatments are available on the market, promising accelerated recovery; however, prolonged use of these medications has been associated with various complications, including hypopigmentation and the appearance of scars [6].

Herbal remedies have gained widespread acceptance as an alternative form of medicine in both developed and developing nations [7]. Factors such as cost-effectiveness, availability, and the trust of local populations have led organizations like the World Health Organization (WHO) and India to endorse traditional medicine practices [8]. Simple herbal remedies have demonstrated efficacy in treating various skin-related conditions and promoting wound healing [9]. Phytoconstituents, active plant extracts, have gained popularity due to their perceived safety, reliability, and minimal adverse effects [10].

Recent research has explored a variety of formulations, including ointments, creams, gels, emulsions, suspensions, liquids, sprays, jelly, carbogels, wet dressings, foams, lotions, and lipogels, all containing herbal ingredients with potential

wound healing properties [11, 12]. While numerous wound creams are under investigation, their ability to significantly accelerate tissue regeneration remains uncertain [13].

Wound healing is a multifaceted process involving the restoration of damaged skin or internal organs. In normal conditions, the skin's epidermal and dermal layers cooperate to maintain a protective barrier against the environment [14]. However, when this barrier is disrupted by injury, a highly orchestrated cascade of intricate biochemical reactions ensues to facilitate wound healing. Following injury, platelets rapidly aggregate at the site, forming a fibrin clot that serves to halt bleeding, a process known as hemostasis. The duration required for wound healing varies widely, depending on various factors, from the time of injury onward [15, 16].

The current study focused on the development of nanogel formulations that contain oleanolic acid-loaded silver nanoparticles. These formulations underwent a rigorous evaluation, including pH determination, viscosity measurement, spreadability analysis, a skin irritancy test, visual inspection, and in vitro and ex vivo drug release, to assess their therapeutic properties. Additionally, Swiss albino rats were employed in this study to investigate the wound-healing potential of topical nanogels containing silver nanoparticles.

2. MATERIALS AND METHODS

Silver nitrate was purchased from Sigma-Aldrich (Germany) from a local vendor. Carbopol 940, were procured from SD Fine Chem Ltd., India. DMSO was sourced from HiMedia Chemicals Ltd., India. Oleanolic acid (>95% purity) was purchased from Yucca Enterprises, and triethanolamine, employed in the experiments, was supplied by the German company Sigma Aldrich Ltd. All analytical-grade chemicals utilized in this study, including double-distilled water, were generated using the Borosil® distilled water apparatus.

2.1. Preparation of Silver Nanoparticles (AgNps)

For the synthesis of AgNPs, a silver nitrate ($AgNO_3$) solution of strength 1 mM was prepared by dissolving 0.01698 g of solute in 100 ml of double-distilled water. An oleanolic acid solution of strength 1 mM was prepared by dissolving 0.04567 g of solute in 100 mL of double-distilled water. Oleanolic acid (5.0 mL) solution was added to 4.0 mM $AgNO_3$ solution at room temperature (25–28°C). The change in color after 30 min showed a rapid reduction of $AgNO_3$ and continued the observation in color change till 24 hr (Table 1) [17].

Table 1: Composition for Silver nanoparticles

Formulation code	Silver Nitrate solution (ml)	Oleanolic Acid(ml)
F1	25	100
F2	25	200
F3	30	100
F4	30	200
F5	35	100
F6	35	200
F7	40	100
F8	40	200
F9	45	100
F10	45	200

2.2. Solid State Characterization of Silver Nanoparticles (AgNps)
2.2.1. UV-Vis Spectroscopic Study

UV-Vis Spectrophotometer (double beam Shimadzu® UV-1800, Kyoto, Japan) in the range of 200–800 nm was used to examine the development of ionic silver's transformation into its corresponding element type. The use of distilled water served as a standard. To verify the AgNPs' production, their absorption peak was calculated [17].

2.2.2. Differential Scanning Calorimetric (DSC) Analysis

To assess the thermal properties of pure oleanolic acid and its silver nanoparticle counterpart, differential scanning calorimetry was performed. Prior to analysis, the moisture content was eliminated through heating. Each sample, weighing approximately 3–7 mg, was accurately placed within a hermetically sealed platinum crucible with a 40-μL aluminum pan. Alpha-alumina powder served as a reference material. Thermograms were recorded within the temperature range of 50°C to 300°C, employing a heating rate of 20°C/min. The measurements were carried out under an inert nitrogen gas atmosphere with a constant flow rate of 20 ml/min.

2.2.3. Scanning Electron Microscopy (SEM)

Surface morphology analysis of oleanolic acid-loaded silver nanoparticles was conducted using a scanning electron microscope with magnifications of 400x and 2000x. For sample preparation, the silver nanoparticles were coated with a 4A° thickness of gold and affixed to aluminum stubs using double-sided tape within the SEM chamber system. Photomicrographs of the developed formulation were captured under an operational accelerating voltage of 6 kV.

2.2.4. *Invitro* Drug Release of Silver Nanoparticles

The *in vitro* drug release profile of the oleanolic acid-loaded silver nanoparticle was carried out using the dialysis bag method. The in vitro release of silver nanoparticles was analyzed using phosphate buffer with a pH of 7.4. The oleanolic acid-loaded silver nanoparticles were transferred to a dialysis bag. The dialysis bag was kept in 100 mL of phosphate-buffered saline at pH 7.4, which is kept under a magnetic stirrer for continuous shaking. A total of 5 mL of the PBS solution was removed from the system and replaced with 5 mL of fresh PBS solution at various time intervals, namely 1, 2, 4, 8, and 12 h, to determine the release of silver nanoparticles. The amount of oleanolic acid released was estimated spectrophotometrically at 248 nm [17, 18].

2.3. Formulation of Oleanolic Acid containing AgNPs Nanogel

Nanogel The nanogel formulation (Table 2) was prepared by combining distilled water, optimized silver nanoparticles (1% w/w), carbopol 940 (0.5 g), and triethanolamine (0.2 ml). The hydrated carbopol 940 gel matrix consisted of distilled water in sufficient quantity, while silver nanoparticles were dispersed in distilled water, which was then added dropwise. Continuous agitation led to gel formation. The permeation enhancer dimethyl sulfoxide (DMSO) was introduced as soon as gel formation commenced, followed by solidification of the gel [19].

Table 2: Formulation Table of Nanogel

Carbopol (g)	0.5
TEA(ml)	0.2
DMSO	60 %
Methyl paraben	0.3 %
Propyl paraben	0.1 %
Distilled water	Quantity sufficientt

2.4. Evaluation of Oleanolic Acid containing AgNPs Nanogel

2.4.1. Physical Assessment

The developed nanogel formulation, denoted as F, underwent comprehensive assessment to evaluate its physicochemical characteristics, encompassing pH, viscosity, and spreadability [20].

2.4.2. pH Measurement

A digital pH meter was employed to determine the pH of the gel formulation (F). Prior to measurement, calibration was performed using buffered solutions at pH 4 and pH 7 to ensure accurate readings. The glass electrode and reference electrode were fully immersed in the gel to obtain precise pH measurements [21].

2.4.3. Spreadability

The evaluation of the formulation's spreadability was conducted using a specially designed apparatus consisting of a flat wooden block with an attached pulley at one end. To assess spreadability, a 2 g portion of each formulation was evenly spread onto a glass slide, and the assessment was based on drag and slip characteristics. The formulation was placed between two slides of identical dimensions, with a hook securing them together. A 50-gram weight was applied to each slide to flatten the film between them and expel any trapped air within the mixture. Any formulation extruding from the margins was removed. The time taken for the upper slide to travel a distance of 7.5 cm was measured using a weighted hook that provided a pulling force of 50 g [22].The following formula was employed to calculate the formulation's dispersibility:

$$\text{Spreadability} = \frac{M \times L}{T}$$

Where:
S = Spreadability (in g·cm/s)
M= Weight tied to the upper slide (50 g)
L = Length of travel (7.5 cm)
T = Time taken to traverse the distance (in seconds)

2.4.4. Skin Irritancy Test

A skin irritancy test was conducted by applying 0.5 g of the formulation to a 6 cm2 area of the skin. The applied formulation was then covered with a gauze piece and secured with a semi-occlusive dressing for a duration of 1 hour. After removal of the gauze and a one-hour observation period, any remaining material was disposed of without altering other conditions. Sensitivity reactions, as well as any signs of irritation or response, were meticulously assessed. Routine and graded observations were made over a 7-day period [23, 24].

2.4.5. Viscosity Measurement

The apparent viscosity of the gel compositions was determined at room temperature and a rotational speed of 50 rpm using a Brookfield viscometer [25].

2.4.6. *Exvivo* Diffusion Cell Study

To assess drug permeability through the biological barrier, Franz's diffusion cells were utilized in the ex-vivo diffusion study. The protocol involved placing the rat abdominal skin in the receptor compartment and securing both compartments firmly with clamps. A phosphate buffer at pH 7.4 served as the receptor solution. Throughout the study, the volume of the diffusion cell was maintained at 6 ml, and magnetic stirring at 100 rpm was maintained using a magnetic bead. The temperature of the entire system was carefully maintained at 37°C ± 1°C using a hot plate. The diffusion study spanned a period of 12 hours, during which 1 ml of samples were cautiously withdrawn at one-hour intervals and subsequently analyzed spectrophotometrically at 248 nm. To ensure a sink condition, an equivalent volume of phosphate buffer (pH 7.4) was added to the receptor compartment after each sample withdrawal.

2.4.7. Accelerated Stability Studies

To assess the stability of the formulation under accelerated conditions, it was subjected to a 180-day testing period at elevated temperature and humidity levels (40 ± 2°C and 75% ± 5% RH). The pharmaceutical preparations were stored in PVC containers with aluminum wrapping. After the 180-day duration outside of the stability chamber, various pharmaceutical properties of the formulations were re-evaluated, including pH, visual appearance, viscosity, and spreadability [28].

2.4.8. Wound Healing Activity

To investigate wound healing activity, rats' tails and hind legs were depilated using a hair removal lotion. The excision method was employed to create a circular wound with a diameter of 10 mm on the experimental rats. A sterile measuring instrument was used to precisely measure the wound size, and the area was demarcated using a black marker. The rats were anesthetized with chloroform in a controlled environment, after which the marked skin section was excised using a No. 18 surgical blade and forceps. Following the incision, the skin was carefully removed, and the wound area was determined between day zero and day fifteen using transparency paper, a ruler, and a measuring tape [18]. The percentage of wound contraction was calculated using the following formula:

$$\textbf{Percentage of wound contraction} = \frac{\textbf{Initial wound size} - \textbf{Specific day wound size}}{\textbf{Initial wound size}} \times \textbf{100}$$

3. RESULTS AND DISCUSSION

3.1. Evaluation of Silver Nanoparticles

3.1.1. UV–Visible spectroscopic study

In order to identify AgNPs, oleanolic acid precipitated the $Ag+$ ions from $AgNO_3$ into their equivalent elemental form. Over the course of 24 hours, the color of the solution changed from clear to dark brown as $AgNO_3$ was reduced to $Ag+$ (Figure 1A). After 24 hours, there should be no more noticeable color change in the solution, indicating that the reduction and AgNPs production have been completed. UV-Vis absorption observations at hourly intervals corroborated the color shift, and absorbance at 440 nm suggested elemental silver form, which peaks at about 24 hrs. Inspired by the interaction with electromagnetic fields, the SPR is a coupled oscillation of free electron conduction. The stimulation of the SPR peak (Figure 1B) may account for the transformation of the clear solution into a dark brown hue during the reduction. The formation of a new absorbance band in the visible region with a maximum at max = 380–750 nm confirmed the initiation of AgNPs production and the advancement of silver ion reduction in solution. The presence of oleanolic acid as a natural capping agent was also indicated by a shift in the SPR band to a strong absorption peak at 440 nm (after 24 hours) [17].
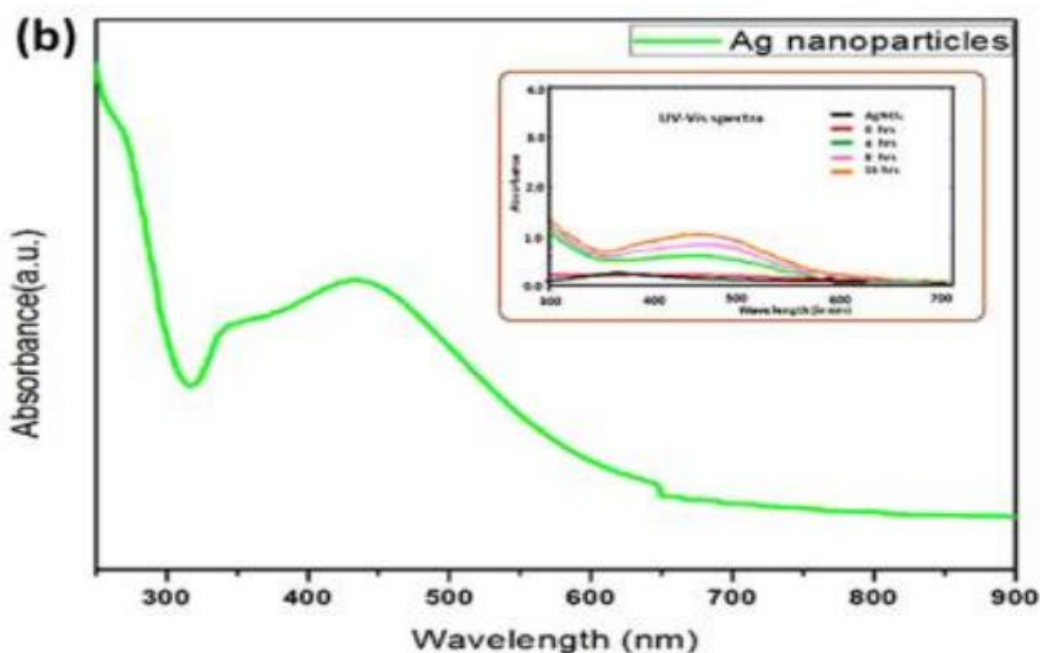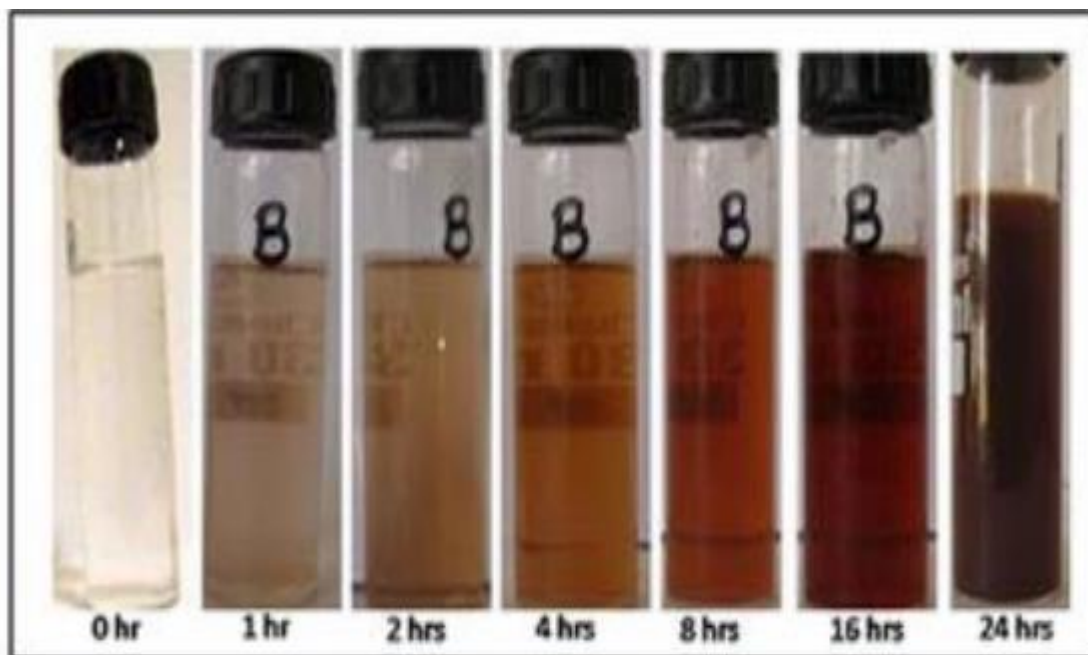
Figure 1. Color change of reaction mixtures UV–Vis absorbance spectra of as prepared AgNPs
at different time intervals: (a) Visual observation (b) UV-Vis absorption spectra

3.1.2. Differential Scanning Calorimetric (DSC) Analysis

The analysis of silver nanoparticles (AgNPs) revealed a distinct endothermic peak at 187.52°C, precisely matching the melting point of oleanolic acid. This sharp peak provided robust confirmation of the crystalline nature of the drug. In the formulation incorporating AgNPs, a noteworthy profile emerged, displaying both a broad endothermic peak and a sharp crystalline peak (Figure 2A) at 85.27°C across the entire scanning range of 30-300°C. This observation indicated the presence of the drug in conjunction with polymers; however, it also suggested a transition of the drug into an amorphous state. Conversely, in the optimized formulation, the absence of sharp peaks (Figure 2B) was conspicuous. Moreover, a notable deviation from the physical mixture was observed, as evidenced by a shift of the endothermic peak to a lower

temperature. This shift implied a rapid transformation into an amorphous state.
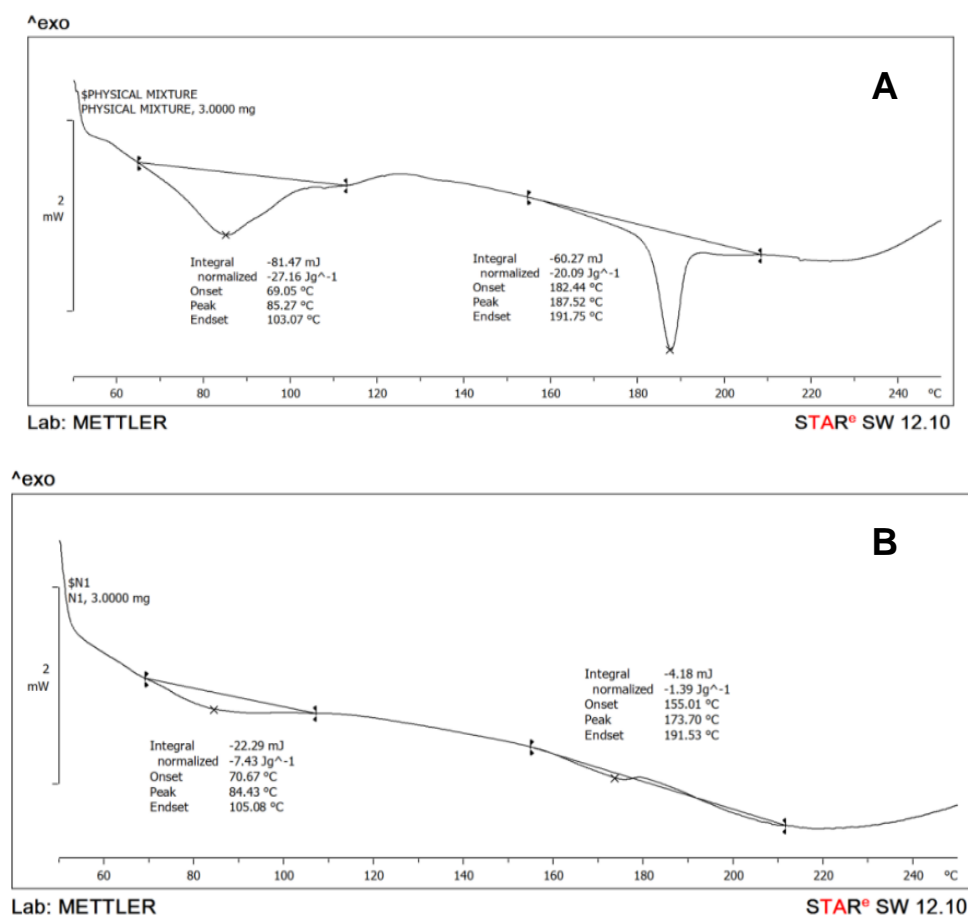
Figure 2. Differential scanning calorimetric (DSC) thermogram: (A) physical mixture; (B) formulation.

3.1.3. Scanning Electron Microscopy (SEM)

The SEM image presented (Figure 3) revealed the hexagonal structure of AgNPs on a plane, whose size ranges from 10 to 50 nm. Additionally, the crystalline nature of the AgNPs was further corroborated by the presence of a well-defined circular diffraction pattern in the targeted region of electron diffraction.
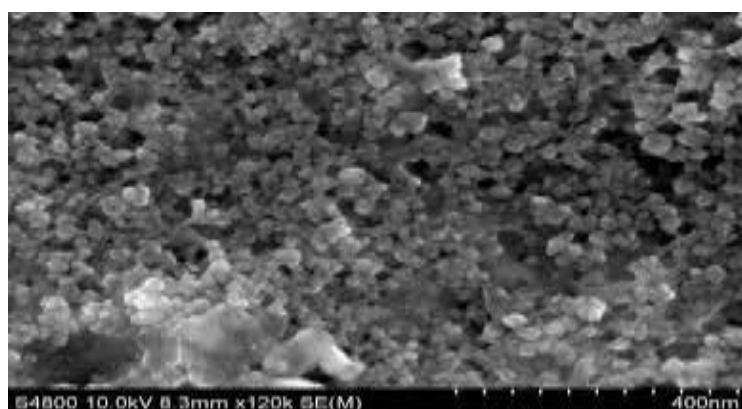
Figure 3. Particle morphology of AgNPs by Scanning Electron Microscope

3.1.4. Zeta potential

The zeta potential was found to be -19.3 mV, which indicated that AgNPs are highly physically stable. Generally, zeta potentials that are more negative than -30 mV or more positive than +30 mV are normally considered stable (Table 3). The zeta potential was observed to be in the partial negative, which may be due to the presence of carboxylic acid,

hydroxyl, and methyl groups in oleanolic acid.

Table 3: Evaluation of Silver nanoparticles

Formulation Code	Entrapment efficiency (%)	Particle size (nm)	Zeta potential (mV)	Drug Release in 12 hours(%)
F1	81.43±2.09	37.44±2.76	-32.04±0.25	78.81±4.82
F2	86.17±3.07	21.56±1.59	-27.5±0.72	73.15±6.32
F3	78.56±0.99	39.71±0.97	-29.64±0.27	68.74±0.78
F4	93.26±1.75	26.13±0.11	-25.14±0.48	60.35±1.87
F5	90.66±3.80	40.16±0.27	-27.21±1.21	63.54±4.42
F6	84.06±9.36	25.12±2.45	-23.64±0.48	66.98±3.83
F7	79.11±3.96	39.68±0.69	-31.04±0.72	74.04±2.25
F8	83.47±2.65	27.09±1.32	-28.84±0.47	75.33±0.89
F9	**94.33±2.03**	**34.24±0.31**	**-19.11±0.34**	**94.77±0.93**
F10	84.69±1.33	29.03±0.12	-26.31±0.34	88.44±0.44

3.1.5. *In vitro* Drug Release of Silver Nanoparticles

The *in vitro* drug release profile of the oleanolic acid-loaded silver nanoparticles was carried out using the dialysis bag method. The *in vitro* release of silver nanoparticles was analyzed using phosphate buffer with a pH of 7.4. In vitro studies were conducted to investigate the drug release profiles of silver nanoparticles (Figure 4). AgNPs exhibited the highest percentage of drug release, reaching 94.77 % after a 12-hour period (Table 4). It is important to note that nanosized carriers play an important role in drug release.
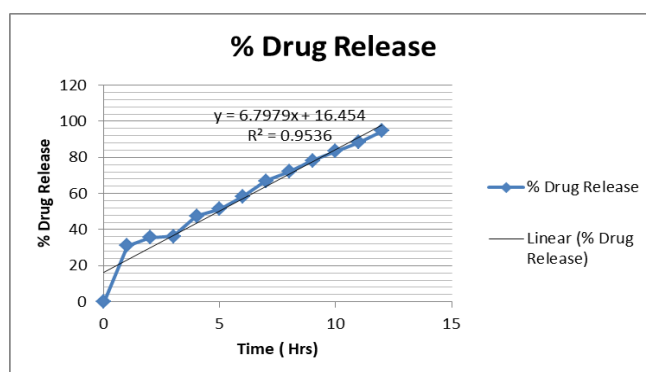

Figure 4. *In - vitro* drug release of Silver nanoparticles (F9)

Table 4. *In - vitro* drug release study of silver nanoparticles F9

Time (Hrs)	% Drug Release
1	30.99
2	35.65
3	36.35
4	47.52
5	51.36
6	58.36
7	66.86
8	72.22
9	78.28
10	83.45
11	88.33
12	94.77

3.2. Evaluation of Nanogel The results evaluation parameters of nanogel formulation mentioned in Table 5

Table 5. Results of various evaluation parameters of nanogel formulations

Sr. No.	Parameters	Observations
1	Appearance	Clear
2	Viscosity (cps)	3500
3	pH	5.5
4	Spreadability(g.cm/sec)	6.9
5	Skin Irritancy test	No rashes and irritation

3.2.1. pH Assessment

The pH values of the formulations were determined for compatibility on dermal application, as they closely align with the typical pH range of human skin, which falls within the range of 5.5. The concentration of triethanolamine increases the pH of the gel.

3.2.2. Spreadability Evaluation

The spreadability of the nanogel formulation was measured at 6.9 g/cm2/sec. This observation is consistent with the principle that as the viscosity of a formulation decreases, its spreadability increases. Formulations exhibited lower spreadability due to their higher viscosity. The increased activity of formulations may be attributed to their high viscosity, resulting in greater retention at the wound site, thereby delivering a concentrated product amount to the wound.

3.2.3. Visual Assessment

Nanogel formulations exhibited an aesthetically pleasing appearance, featuring a colored, velvety texture that felt soft to the touch. They were devoid of grittiness, caused no irritation, and exhibited no noticeable defects. The formulation appeared as greenish-brown gels with a characteristic herb-like aroma. In terms of visual appeal, this formulation exhibited a more elegant appearance than other formulations.

3.2.4. Skin Irritation Testing

During the skin irritation test, no signs of edema or erythema were observed following consecutive 7-day applications. Notably, the optimized formulation demonstrated a lower potential for skin irritation compared to other formulations. This observation is significant in the context of product compatibility for human use. Unlike many synthetic cosmetics on the market that may contain new synthetic excipients leading to skin irritation in sensitive individuals, formulations exhibited superior compatibility, causing no local irritation.

3.2.5. Viscosity Measurement:

In the evaluation of the rheological properties of the formulations, the viscosity was determined to be 3500 cps. It is noted that carbopol 940 increases the viscosity due to high cross-linking. The higher viscosity of the formulation contributes to prolonged product retention on the wounded surface, ensuring sustained therapeutic action over time.

3.2.6. Ex vivo diffusion studies of Nanogels

Ex vivo diffusion studies of Nanogels were conducted to investigate the drug diffusion profiles of nanogel formulations (Figure 5). Formulation exhibited the highest percentage of drug diffusion, reaching 84.66 % after a 12-hour period (Table 6). It is important to note that aside from the inherent properties of the polymer, the concentration of the polymer also played a role in affecting drug release. An increase in polymer concentration corresponded to a decrease in drug release. Due to the presence of cross-linking of polymers, the nanogel formulation has shown a delay in drug release as compared to silver nanoparticles.
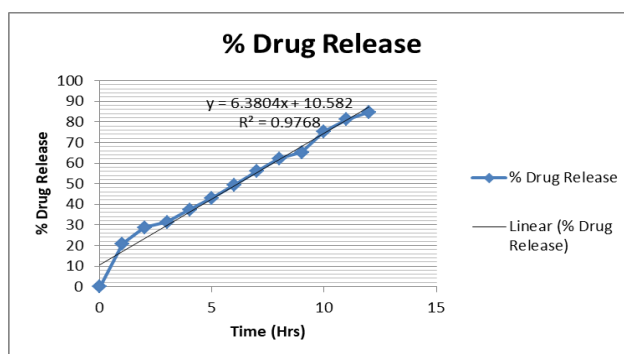

% Drug Release

$y = 6.3804x + 10.582$
$R^2 = 0.9768$

Figure 5. *Ex-vivo* drug diffusion study of Nanogel

Table 6. *Ex - vivo* drug diffusion study of nanogel

Time (Hrs)	% Drug Release
1	20.77
2	28.68
3	31.35
4	37.31
5	43.06
6	49.39
7	56.06
8	62.20
9	65.15
10	75.38
11	81.23
12	84.66

3.2.7. Accelerated Stability Assessment

During the accelerated stability study conducted on the product under conditions of 40°C ± 2°C and 75% ± 5% relative humidity over a duration of 180 days, the formulated nanogel preparation exhibited minimal alterations in its physical characteristics. These included aspects such as appearance, viscosity, spreadability, and pH, as depicted in Table 4. It is noteworthy that the optimized formulation displayed greater resilience with respect to the physical characteristics of freshly prepared nanogel (Table 7), suggesting effective preservation of the formulation's integrity under accelerated stress conditions. Consequently, the prepared nanogel formulations demonstrated a high degree of stability throughout the study period.

Table 7. Results of accelerated stability studies of nanogel formulations

Parameters	Before Storage	After 180 days
Appearance	Clear	No change
Spreadability (g.cm/sec)	6.9	6.6
pH	5.5	5.4
Viscosity (cps)	3500	3450

3.2.8. Wound Healing Evaluation

The wound healing efficacy of the formulation was investigated using Swiss albino rats (Figure 6). Initially, on day zero, prominent scarring was observed on the dorsal region of the experimental animals. Subsequent to the application of formulation (F) with standard (S) to the wounded areas, a visible reduction in scar prominence was observed following extended applications on the 1st day (F = 0%, S = 0%), 3rd day (F = 11.53 %, S = 10.71%), 6th day (F = 46.37 %, S = 39.28%), 9th day (F = 65.38 %, S = 64.43%), 12th day (F = 88.46 %, S = 87.24%), and 15th day (F = 99.15%, S = 95%) (Table 8). Silver nanoparticles are believed to play a pivotal role in enhancing wound healing in Swiss albino rats by significantly accelerating the rate of wound closure, migration, and epithelization. Formulation exhibited superior activity compared to standard, and several factors contribute to this phenomenon. Firstly, pharmaceutical properties such as viscosity and spreadability enable better product concentration at the wound site, facilitating enhanced interaction with scar tissue components. Silver nanoparticles possess pharmacokinetic-modifying properties that promote efficient epithelization. Moreover, these nanoparticles contain various known and unknown chemical constituents that exert significant pharmacological, pharmacodynamic, and pharmacotherapeutic effects on wound healing.

In comparison to the standard drug betadine, the formulation demonstrated similar efficacy. Figure 5 illustrates the visual progression of wound healing and reduction in wound contraction over the course of 15 days for formulations as well as the standard drug betadine.

Table 8. Effect of nanogel on excision wound healing

Group	% Wound Contraction					
	1st Day	3rd Day	6th Day	9th Day	12th Day	15th Day
Standard	0%	10.71%	39.28%	64.43%	87.24%	95%
Formulation	0%	11.53%	46.37%	65.38%	88.46%	99.15%

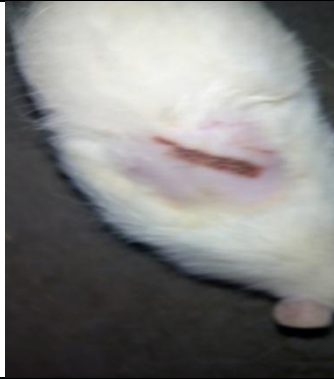**Figure 5.** *Ex-vivo* drug diffusion study of Nanogel

DAY	STANDARD (S)	FORMULATION (F)
1st		
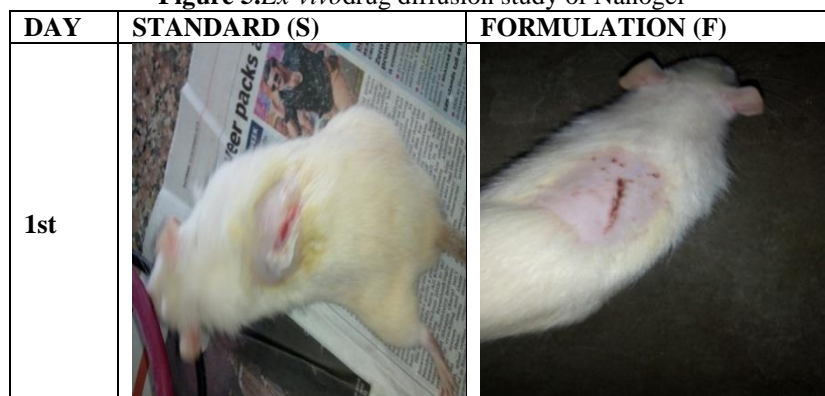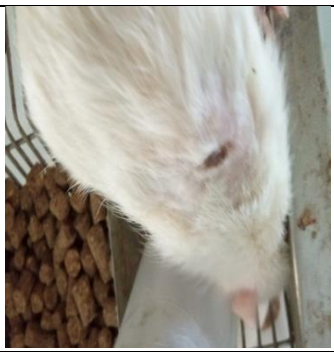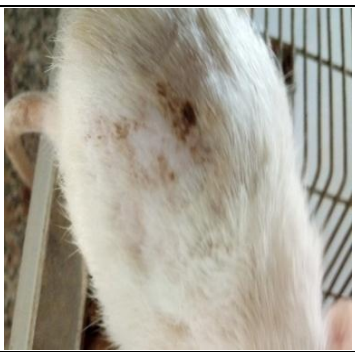
Figure 6. Day-wise progress of wound healing in experimental animals

4. Conclusion:

The results of this study show that the formulation was prepared by using carbopol 940 and triethanolamine. The parameters were analyzed as pH 5.5, viscosity 3500 cps, spreadability 6.9 g/cm/sec, and there was no skin irritation. In vitro drug release studies showed a release rate of 94.77 % in 12 hours. *Ex-vivo* drug release has shown slow drug release as compared to silver nanoparticles, which had 84.66% drug release in 12 hours due to the presence of high cross-linking polymers. The wound healing capabilities of topical gel containing silver nanoparticles showed almost the same results as marketed betadine topical cream. Stability studies of nanogel formulation confirmed the spherical shape and uniform particle size of silver nanoparticles and the good stability of nanogel. This study has promising avenues for the treatment of wounds originating from various sources. The formulated wound healing gel formulation containing silver nanoparticles holds potential for future applications as a wound healing agent, facilitating the acceleration of natural wound healing processes

ETHICS APPROVAL AND CONSENT TO PARTICIPATE

This protocol received approval from the Institutional Animal Ethical Committee of Dr. Rajendra Gode College of Pharmacy, Malkapur (MH).

REFERENCES

1. Ramteke C, Chakrabarti T, Sarangi B & Pandey R. (2013).*J. Chem.* 278925: 7.
2. Rani P & Rajasekharreddy P. (2011) *Physicochem Eng Aspects*.389:188–94.
3. Rao C, Müller A & Cheetham A.(2006)*John Wiley & Sons.*
4. Rao C, Müller A & Cheetham A.(2006) John Wiley & Sons.
5. Rao K & Paria S. (2010) Mater. Res. Bull.
6. Rao M & Savithramma N.(2012) *Res. Biotechnol*. 3(3):41-47.
7. Rao M & Savithramma N.(2011) *J. Pharm. Sci. and Res.* 3(3):1117-21.
8. Rao Y, Kotakadi V, Prasad T, Reddy A & Gopal D. (2013) *Mol. Biomol. Spectr*.103:156–9.
9. Rao P, Chandraprasad M, Lakshmi Y, Rao J, Aishwarya P & Shetty S. (2014) *Int J. Multidisip. Res. Dev*.2:165-9.
10. Raut R, Kolekar N, Lakkakula J, Mendhulkar V & Kashid S. (2010) *Nano-Micro Lett. 2:106-13.*
11. Renugadevi K, Inbakandan D, Bavanilatha M & Poornima V. (2012)Int J Pharm Bio Sci. 3(3):437–45.
12. Renugadevi K, Aswini V & Raji P. (2012) *Asian J Pharm Clin Res.* 5(4):283-7.
13. Resmi C, Sreejamol P & Pillai P. (2014) *Int J Adv Biol Res*. 4(3):300-3.
14. Rodríguez-León E, Iñiguez-Palomares R, Navarro R, Herrera-Urbina R, Tánori J, Iñiguez-Palomares C & Maldonado A. (2013) *Nanoscale Res. Lett.* 8:318.
15. Roopan S, Rohit, Madhumitha G, Rahuman A, Kamaraj C, Bharathi A & Surendra T.(2013) *Indus. Crops and Products.* 43:631–35.
16. Rout Y, Behera S, Ojha A & Nayak P. (2012) *J. Microbiol. Antimicrob*. 4(6):103-9.
17. Shivhare R. & Jain N. (2023) *Eur. Chem. Bull*. 12(8), 2863-2876.

18. Shivhare R & Jain N. (2023) *Bio. Biotech. Res. Asia.* 20 (3).
19. Rupaisih N, Aher A, Gosavi S & Vidyasagar P. (2015) *Recent Trends in Physics of Material Science and Technology.* 1-10.
20. Sable N, Gaikwad S, Bonde S, Gade A & Rai M. (2012)*Bioscience.* 4(2):45-49.
21. Sadeghi B & Gholamhoseinpoor F. (2015)*Spectrochimica Acta Part A* 2015;134:310-15.
22. Sahu N, Soni D, Chandrashekhar B, Sarangi B, Satpute D & Pandey R(2013). *Bioprocess Biosyst Eng.* 36:999–1004.
23. Sahu S, Zheng J, Graham L, Chen L, Ihrie J, Yourick J & Sprando R. (2014) *J Appl Toxicol.* 34:1155–66.
24. Salunkhe R, Patil S, Patil C & Salunke B. (2011) *Parasitol Res* 2011;109:823–31.
25. Sana S, Badineni V, Arla S & Boya V. (2015)*Mat. Lett.* 145:347–50.
26. Sanghi R & Verma P.(2009)*Bioresour Technol.* 100:501.
27. Sankar R, Karthik A, Prabu A, Karthik S, Shivashangari KS & Ravikumar V. (2013) *Colloids Surf B.* 108:80–84.
28. Santhoshkumar T, Rahuman A, Rajakumar G, Marimuthu S, Bagavan A & Jayaseelan C (2011) *Parasitol Res.* 108:693–702.